



HAL
open science

Pluri-decennial erosion rates using SUM/ISUM and sediment traps survey in the Mercurey vineyards (Burgundy, France)

Mathieu Fressard, Etienne Cossart, Brian Chaize

► To cite this version:

Mathieu Fressard, Etienne Cossart, Brian Chaize. Pluri-decennial erosion rates using SUM/ISUM and sediment traps survey in the Mercurey vineyards (Burgundy, France). *Geomorphology*, 2022, 403, pp.108181. 10.1016/j.geomorph.2022.108181 . hal-03767503

HAL Id: hal-03767503

<https://hal.science/hal-03767503>

Submitted on 2 Sep 2022

HAL is a multi-disciplinary open access archive for the deposit and dissemination of scientific research documents, whether they are published or not. The documents may come from teaching and research institutions in France or abroad, or from public or private research centers.

L'archive ouverte pluridisciplinaire **HAL**, est destinée au dépôt et à la diffusion de documents scientifiques de niveau recherche, publiés ou non, émanant des établissements d'enseignement et de recherche français ou étrangers, des laboratoires publics ou privés.

1 Pluri-decennial erosion rates using SUM/ISUM and sediment traps
2 survey in the Mercurey vineyards (Burgundy, France)

3 Mathieu Fressard¹, Etienne Cossart², Brian Chaize²

4 ¹Univ. Lyon, University Lumière Lyon 2, UMR 5600 CNRS-Environnement Ville Société – LYON, F-69007,
5 France.

6 ²Univ. Lyon, University Jean Moulin Lyon 3, UMR 5600 CNRS-Environnement Ville Société – LYON, F-
7 69007, France.

8 **Highlights**

- 9 - SUM/ISUM and sediment traps were used to estimate soil erosion on a vineyard sub-catchment
10 - The mean erosion rate on plots (SUM/ISUM) was $21.4 \pm 3.1 \text{ t.ha}^{-1}.\text{yr}^{-1}$, but varied from -3.2 ± 1.5
11 $\text{t.ha}^{-1}.\text{yr}^{-1}$ to $53 \pm 5.8 \text{ t.ha}^{-1}.\text{yr}^{-1}$.
12 - Sediment accumulation rates in traps varied from 16.6 ± 5.9 (upslope) to 0.13 ± 0.05 (downslope)
13 - The method was affected by error margins (from 7% to 43% of the measured value) that directly
14 correlated with the erosion rate.
15 - Both topography (slope) and agricultural practices (backfilling) were identified as contributing
16 factors of soil erosion.

17

18

19

20

21

22 **Abstract**

23 Vineyards are often considered to be among the agricultural lands most sensitive to erosion. We used
24 the Stock Unearthing Measurement/Improved Stock Unearthing Measurement (SUM/ISUM) method
25 and sediment traps volume measurements to assess the pluri-decennial erosion rates on a sub-
26 catchment of the Mercurey vineyards in Burgundy, France. The measured erosion rates were
27 compared to local environmental conditions (such as slope, soil type, age of vines, etc.) to discuss the
28 role of driving factors. We found that the mean erosion rate was $21.4 \pm 3.1 \text{ t}\cdot\text{ha}^{-1}\cdot\text{yr}^{-1}$ on vine plots
29 (from $-3.2 \pm 1.5 \text{ t}\cdot\text{ha}^{-1}\cdot\text{yr}^{-1}$ to $53 \pm 5.8 \text{ t}\cdot\text{ha}^{-1}\cdot\text{yr}^{-1}$), while sediment accumulation rates in traps varied
30 from 16.6 ± 5.9 (upslope) to 0.13 ± 0.05 (outlet). The measurements were characterized by variable
31 error margins (from 7% to 43% of the measured value) that are directly correlated with erosion rates.
32 Both slope (USLE-LS factor) and age of vines were identified as driving factors of soil erosion. Runoff is
33 the main modality of erosion. The higher erodibility of soil during the first years after plantation
34 (unconsolidated and bare soil); and the regular (every 15 to 20 years) backfilling of eroded plots with
35 soil collected in downslope sediment traps can explain the effect of the age of vines on erosion. In spite
36 of erosion control strategies, the measured rates remain higher than what can be tolerated for
37 sustainable development of agriculture. Therefore, we suggest that the current erosion mitigation
38 strategy should be complemented with other techniques that maintain soils on plots (e.g., grass strips
39 on the interrows, mulching).

40

41

42

43

44

45

46 **1. Introduction**

47 Vineyards are among the agricultural lands most sensitive to erosion (Kosmas et al., 1997; Cerdan et
48 al., 2010; García-Ruiz et al., 2015). In French vineyards, measured erosion rates range from 10.5 to 54
49 t.ha⁻¹.yr⁻¹ (Viguié, 1993; Quiquerez et al., 2008; Paroissien et al., 2010; Prosdocimi et al., 2016). While
50 erosion rates measured in Burgundy are of intermediate level, ranging from 14 to 23 t.ha⁻¹.yr⁻¹ (Brenot
51 et al., 2008; Quiquerez et al., 2008; Fressard et al., 2017), they remain well above the average reference
52 level of approximately 3 t.ha⁻¹.yr⁻¹ established for all agricultural activities (Cerdan et al., 2006), and
53 values ranging from 0.3 to 1.4 t.ha⁻¹.yr⁻¹ established for soil sustainability (Verheijen et al., 2009).
54 Beyond its direct impact on agricultural yield, the indirect consequences of this erosion threaten the
55 sustainable exploitation of natural resources, causing mudflows, alteration of water quality, transfer
56 of pesticides to rivers, and other consequences on ecosystem-services (eutrophication, biodiversity,
57 carbon storage) (Greene et al., 1994; Pimentel et al., 1995; Lal, 1998; Hildebrandt et al., 2008; Rabiet
58 et al., 2010).

59 Several methods have been developed and applied to measure soil erosion rates in vineyards. These
60 methods are based on a wide variety of techniques and provide estimates of soil erosion at different
61 spatial and temporal resolutions. Direct measurements have been conducted on experimental plots,
62 especially to provide estimates of soil erosion rates under controlled or natural rainfall conditions in
63 real in-field situations (Messer, 1980; De Figueiredo et al., 1998; Battany and Grismer, 2000; Arnaez et
64 al., 2007; Biddoccu et al., 2016; Rodrigo-Comino et al., 2016a). Other techniques for indirect
65 measurements are based on quantification of topographic changes to infer soil erosion. These
66 methods aim to estimate the eroded volumes caused by rilling or gullyng after high intensity rainfall
67 events, doing so by using high resolution Digital Elevation Models (DEMs) obtained from in-field
68 topographic surveys (Martínez-Casasnovas et al., 2002) or high resolution images taken before and
69 after extreme events (Quiquerez et al., 2008; Remke et al., 2018). All of these techniques can provide
70 measurements of erosion rates over relatively large areas (hillslope or small sub-catchment scale), but

71 can only be applied at very short time-scales (e.g., a few years), and cannot account for past erosion
72 processes. To provide information on multi-decennial timescales, radionuclides (Cs 137) have been
73 tested in vineyards (Loughran and Balog, 2006). This method can provide estimates of soil erosion, but
74 it is time consuming and is affected by large uncertainties (Boardman, 2006). Brenot et al. (2008)
75 developed a method called Stock Unearthing Measurement (SUM) that uses the vine stock graft union
76 as a passive marker of former topsoil level. This method allows estimation of eroded and accumulated
77 volumes by comparing the actual distance of the graft union from the ground with a known reference
78 level at the time of vineyard planting. The average erosion rate over multi-decennial timescales can
79 then be calculated, depending on the age of the vines (from 10 to 80 years). The SUM is simple to apply
80 and can provide results at the intra-plot scale with moderate error margins. This method was
81 successfully applied in various vineyards in Europe in the 2010s (Brenot et al., 2008; Casalí et al., 2009;
82 Paroissien et al., 2010b; Rodrigo-Comino et al., 2016a; Fressard et al., 2017). Rodrigo-Comino and
83 Cerdà (2018) proposed an improvement to the method called 'Improved Stock Unearthing
84 Measurement' (ISUM), which considers the fact that the interrows are often more incised than the
85 vine rows themselves. Consequently, a correction factor may be applied to correct former erosion
86 studies that used the SUM method.

87 Collectively, these studies help in the identification of factors contributing to soil erosion in vineyards:
88 topographic factors such as steep slopes (Rodrigo-Comino et al., 2017a), soil erodibility (Le Bissonais
89 et al., 2006), rainfall erosivity (mostly extreme rainfall) (Martínez-Casasnovas et al., 2002; Quiquerez
90 et al., 2008; Ramos and Martínez-Casasnovas, 2009), and factors linked to agricultural practices such
91 as bare soils (Morvan et al., 2014; Napoli et al., 2017), slope oriented rows (Brenot et al., 2008), tillage,
92 and use of herbicides (Salome et al., 2014; García-Díaz et al., 2017). Additionally, Rodrigo-Comino et
93 al. (2018a) showed that the age of vines may influence the level of soil erosion, as terracing and tillage
94 conducted before the planting of new vines and during the first years of vine development increase
95 the sensitivity of soil to erosion. Following such studies, the specific roles of identified controlling
96 factors remain to be discussed and hierarchized.

97 One main scientific debate focuses on the consequences of the backfilling of ephemeral gullies, rills or
98 full plots applied to compensate for soil loss. These practices have been documented in open field
99 cultures in Belgium, and in vineyards in Spain, France, and Germany (Poesen, 1993; Martínez-
100 Casanovas et al., 2005; Quiquerez et al., 2008; Kirchhoff et al., 2017; Fressard et al., 2017). However,
101 it remains difficult to estimate the precise level of compensation and the general role of these human
102 interventions on soil erosion rates. Garcia et al. (2018) used detailed historical registries to provide
103 estimates of anthropogenic compensations in burgundy during the middle-ages. Their study showed
104 that backfilling (manual at that time) could return up to $9 \text{ t}\cdot\text{ha}^{-1}\cdot\text{yr}^{-1}$ of soils over time periods from 25
105 to 39 years. Nowadays, soil backfilling is no longer registered, and it is more difficult to get accurate
106 quantification of anthropogenic practices. However, these practices are still applied, even though their
107 role is not assessed and their efficiency few discussed.

108 In this paper, we contribute to the current debates on the evaluation of the role of specific local
109 controlling factors on soil losses and more particularly on the role of anthropogenic practices
110 (sediment backfilling). We focus on an intensive vineyard sub-region of burgundy, the Mercurey
111 terroir. This sub-region is known for severe soil loss, and vine growers there have developed a
112 collective strategy using sediment collectors and backfilling to mitigate soil loss and the transfer of
113 particles to rivers (Fressard and Cossart, 2019). Using the SUM/ISUM method and volume
114 measurements from sediment traps, we aimed to compare erosion rates between various physical
115 settings, to hierarchize local controlling factors on pluri-decennial erosion rates.

116 **2. Study area**

117 **2.1. Geomorphological context**

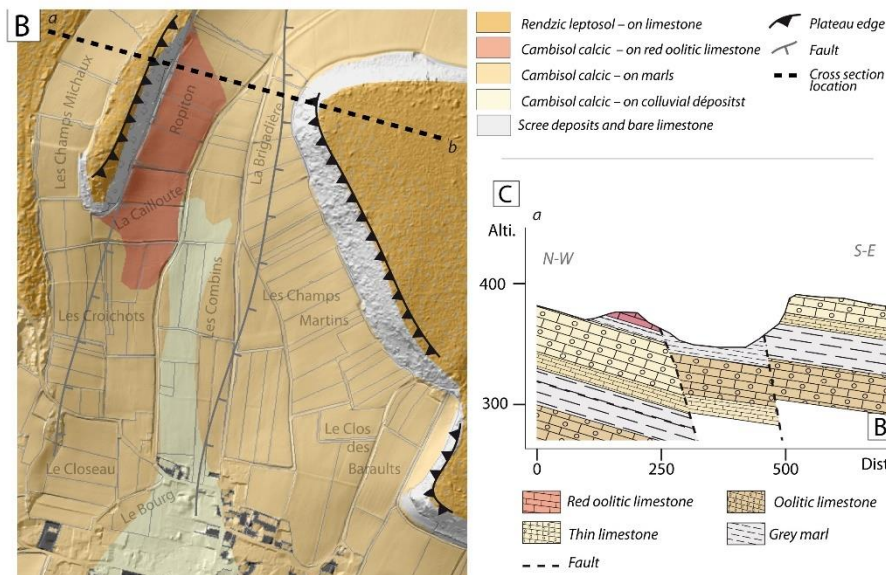
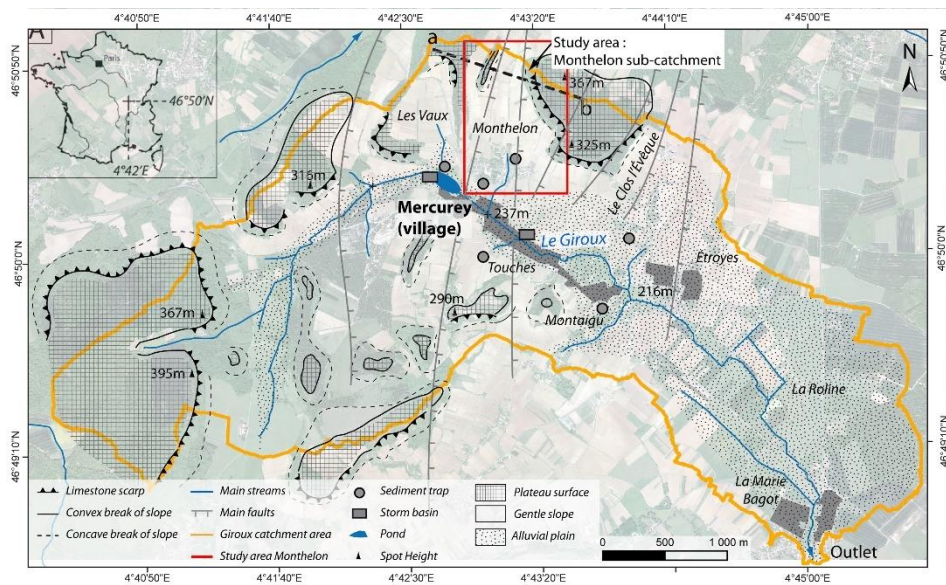
118 The study area is located in the Mercurey terroir, which is part of the Burgundy wine region. The local
119 geology consists of alternations of limestones and marly-limestones organized along tilted blocks
120 dropping from west to east along eight main faults. At regional scale, this complex fault system consists
121 in a contact area between the Morvan massif horst (west) and the Saône plain graben (east), (Fressard

122 et al., 2017). The Mercurey area is characterized by a 2 to 3 km-wide valley drained by the Giroux River,
123 and is subdivided into eight sub-catchments. The measurements were conducted on the Monthelon
124 sub-catchment, located in the northern part of Mercurey (Fig. 1). This sub-catchment is compact, and
125 the global drainage direction is southerly. The vines are planted on gentle to moderately sloping
126 gradients from 5° to 20°, and are surrounded by two steeper calcareous rocky ledges (30° to 40°) with
127 an altitude difference of 15 to 25 m.

128 The mean annual precipitation is 770 mm.yr⁻¹, as measured by the Mercurey weather station (since
129 1971). The months of August and September are characterized by higher precipitation records than
130 other months (80 mm on average) because of storm events and associated intense rainfall: 14 of the
131 18 storm events recorded from 1971 to 2018 (> 50 mm in one day) occurred during these two months.

132 All soils of the catchment are derived from the calcareous rocks that dominate the Mercurey area
133 (limestone and marls). The most frequent soil type is calcosoil (FAO calcic cambisol), which develops
134 on the marls. This soil type is characterized by varying degrees of stoniness (from 30% to 70%), with
135 proximal ledges feeding the surface with scree and debris. These soils are of a moderate thickness (60
136 to 100 cm) and constitute the most frequent type of soil in the Mercurey vineyards. A slight variation
137 in this soil can be observed on the north-west hillslope of the catchment where the upslope red oolitic
138 limestone outcrop delivers a more reddish color to the ground surface (stoniness is also high, ranging
139 from 30% to 60%, and depth is comparable to the most frequent soil type). On colluvial-deposit, soil
140 profiles tend to be thicker (from 1 to 1.5m) still on calcic cambisols. The limestone plateau surface is
141 covered by rendisols (FAO rendzic leptosol). These soils are thin (less than 40 cm), are characterized
142 by a lower carbonate content, and are rarely used for vine cultivation.

143



144

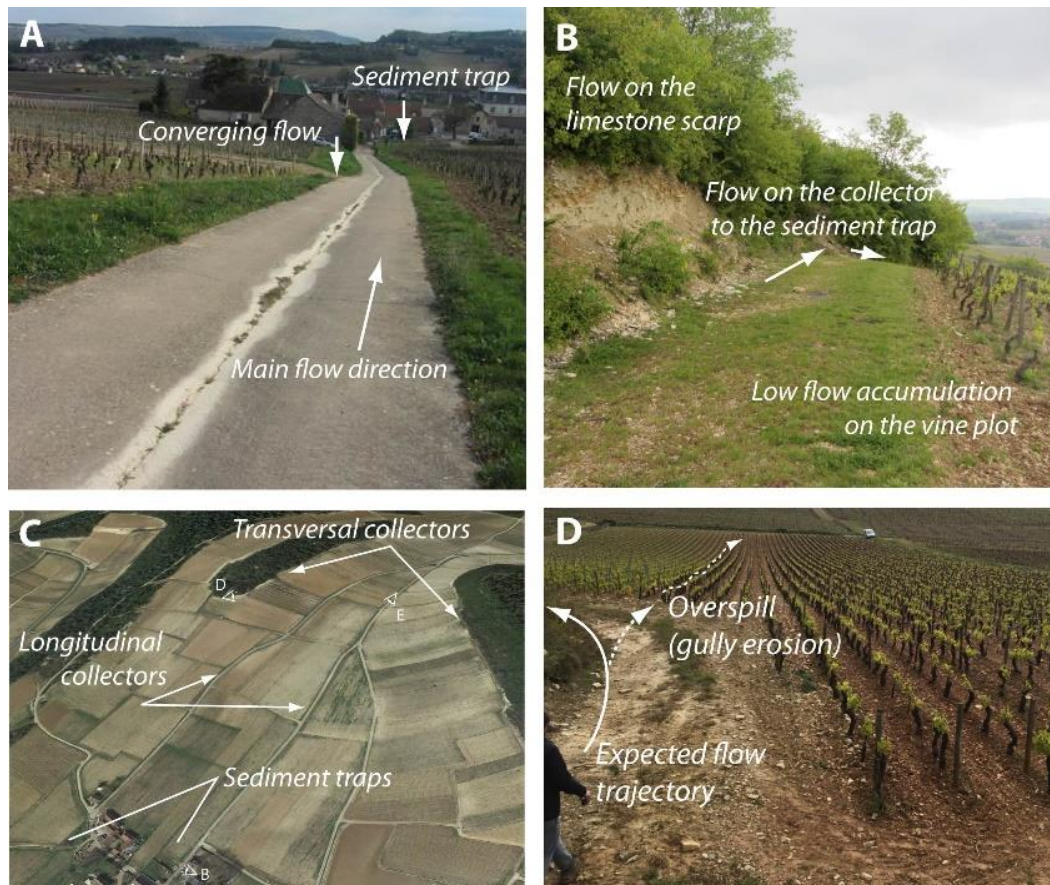
145 *Figure 1: Location of the Monthelon sub-catchment and its pedo-geomorphological context. (A)*
 146 *Geomorphological sketch of the catchment, (B) soil map of the Monthelon sub-catchment, (C)*
 147 *geological cross section of Monthelon, and (D) global location in France.*

148

149 **2.2. Soil erosion management infrastructure and sediment collectors**

150 After a significant phase of economic growth in the 1950s and 1960s, the initial patchwork of grassland
 151 and vineyards turned to almost a monoculture of vines (the surface area devoted to vineyards doubled
 152 after the second world war). Between 1948 and 1976, several hyperconcentrated flows occurred

153 following intense rainstorms (ungauged at that time), but it took the extreme events of 1981 and 1983
154 to raise collective awareness of the problem of soil erosion (Fressard et al., 2017; Cossart et al., 2021).
155 The extreme flood of August 10, 1981 involved a record amount of rainfall (119.5 mm of rainfall in one
156 day) and caused significant damages (destroying roads, flooding approximately 40 houses, and
157 destroying harvests).



158
159 *Figure 2: Examples of infrastructure collecting hydro-sedimentary fluxes on the Monthelon catchment.*
160 *(A) Longitudinal collector, (B) transversal collector, (C) oblique aerial view of the catchment showing*
161 *the organization of the collectors and ground locations, (D) example of overspill from a collector to a*
162 *plot.*



163

164 *Figure 3: Illustrations of the backfilling strategy. (A) Sediment trap, (B) trapped sediments, (C)*
 165 *mechanical filling of parcels with trapped sediments, and (D) result of the backfilling on soil.*

166

167 After another lower magnitude flood on the 12th of September 1983 (59 mm of rainfall in one day), an
 168 association was formed to bring together the grape growers of the Mercurey appellation with the
 169 objective of coordinating soil conservation and flood mitigation efforts. This association had two main
 170 goals: (1) to simplify the parcel pattern geometry, and (2) to take advantage of these simplifications to
 171 develop a network of hydraulic structures to collect and trap sediments. Three types of structures were
 172 built (Figs. 2 and 3) (Fressard and Cossart, 2019). First, on the upper slopes, a network of hedges and
 173 counter-slope paths were used to hamper the hydro-sedimentary flow between the plots and the
 174 upslope plateau edge. Second, ditches were constructed downstream to drain overflowing water and

175 sediments. The objective was to reduce runoff on plots in the middle of the slope, and thus limiting
176 soil erosion. On the lower parts of the hillslopes, "V"-shaped concrete roads force the flow to converge
177 towards the basins, in the direction of sediment traps (Fig. 2). The aim of these traps was to collect the
178 sediments removed from the plots before they were exported to the Giroux River. If the sediments are
179 thus captured, soil backfilling can be performed on the plots using the trapped sediments (Fig. 3).
180 Interviews with the grape growers revealed that backfilling is generally performed every 15 to 20 years
181 on sloping vineyards, and more frequently on areas (vine rows) specifically affected by gullies.

182

183 **3. Methods**

184 **3.1. SUM measurements**

185 **3.1.1. General principle**

186 The Stock Unearthing Method (SUM) developed by Brenot et al. (2006; 2008) has been widely used to
187 estimate soil erosion in European vineyards (Brenot et al., 2008; Casalf et al., 2009; Paroissien et al.,
188 2010a; Rodrigo-Comino et al., 2016, 2018a, 2018b). This method is based on the unearthing of the vine
189 stock from the graft union, which is presumed to be spatially immobile in three dimensions. The graft
190 union is thus considered a passive marker of soil erosion. Since the Phylloxera crisis in the 19th century,
191 most European vines are grafted onto American stocks (underground roots), which are the only grape
192 variety able to resist the pest. For agronomic reasons, the graft union point is systematically placed 1
193 or 2 cm above the ground when planting young vines. This *a priori* initial height is variable depending
194 on bibliographical sources (e.g. 1 cm for Brenot et al., 2008 and 2 cm for Paroissien et al., 2010 and
195 Rodrigo-Comino et al., 2018). The absolute position of this point is affected by a limited downwards
196 shifting through time (Reynier, 2011) that has been quantified to be 0.2 mm.yr⁻¹ by Brenot et al. (2008)
197 for pinot noir varietal (varietal grown in Mercurey). Measurement of the distance between the graft
198 union and the ground allows deduction of the ablation rate on each vine plant. By repetitively applying

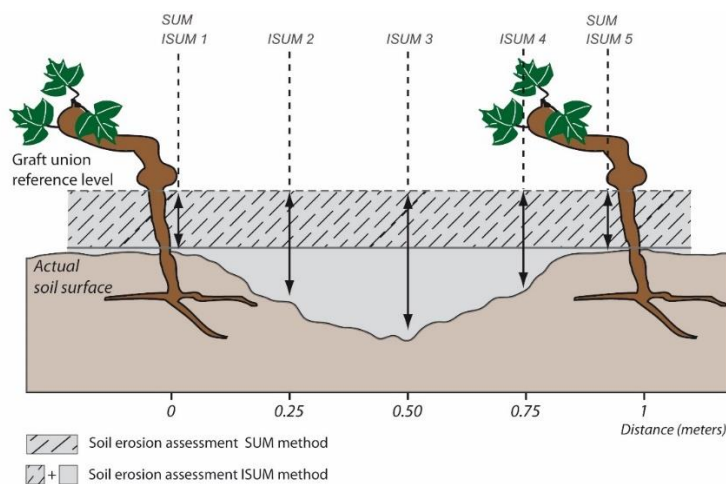
199 this measurement on experimental plots, the method allows the spatial patterns of erosion dynamics
 200 to be estimated according to formula A:

$$201 \quad ER = \frac{Vol \times D_s}{S_t \times A_v}$$

202 where, ER is the erosion rate expressed in $t \cdot ha^{-1} \cdot yr^{-1}$, Vol is the estimated eroded volume, D_s is the soil
 203 bulk density, S_t is the surface area, and A_v is the age of the vine plot.

204 **3.1.2. ISUM corrections**

205 The ISUM method (Rodrigo-Comino and Cerdà, 2018) involves the acquisition of measurements in the
 206 interrows, which are known to be more affected by erosion and tractor compaction. Additionally, the
 207 practice of ridging and un-ridging the vine rows is frequent in viticulture, and tends to artificially reduce
 208 the gap between the graft union and the ground on the vine row, whereas the interrow is artificially
 209 deepened. Measurements are conducted along a string stretched between two vine plants graft unions
 210 (or at a specific distance from the graft union on the plant) located on either side of the interrow (Fig.
 211 4). This technique is very similar to that using erosion pin meters, which are widely used to measure
 212 soil roughness or to map gully erosion volumes (e.g. Casalí et al., 2006). Further details on the practical
 213 application of ISUM are provided in section 3.1.3.



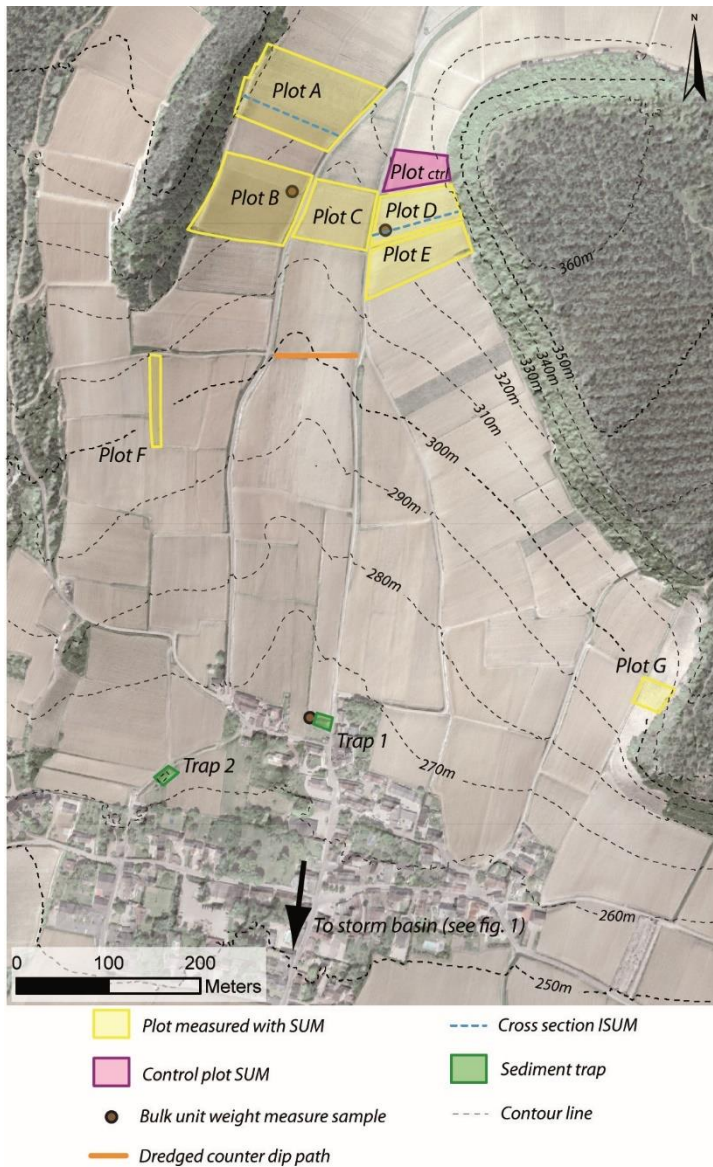
214
 215 Figure 4: Illustration of the general principles of SUM and ISUM (after Brenot et al., 2008; and Rodrigo-
 216 Comino and Cerdà, 2018).

217 **3.1.3. Field measurements and sampling strategy**

218 We used the classical SUM method to measure 2359 vine plants over seven plots in the sub-catchment
219 of Monthelon (plots referred to as A–G; Fig. 5), which consists in manually measuring with a ruler the
220 distance between the graft union and the soil (given in cm with a 0.5 cm accuracy as suggested by
221 Brenot et al., 2008). To minimize the errors that can arise from soil roughness (effect of tillage and
222 stoniness), measurements were performed systematically on the downhill side of stocks and
223 conducted in winter (as suggested by Brenot et al., 2008 and Paroissien et al., 2010). The main
224 objective was to estimate the erosion rates on different types of parcels representing the diversity of
225 the topographic characteristics of the area (steep to long and gentle slopes), as well as the various ages
226 of the vine plants (from 9 to 42 years). In the investigated plots, measurements were made at a
227 sampling distance of every 2 rows and every 3 plants in-row. This returned regular nodes on a gridding
228 of 3 x 3 m. The positions of all measured vine stocks were determined by differential GPS with a
229 centimetric x, y, z accuracy. The z values (altitude) were not used for volumetric calculations as the
230 GPS vertical accuracy (centimetric) is beyond what is requested by SUM.

231 To provide maps of the spatial distribution of erosion rates, we performed a spatial interpolation of
232 the measured SUM values. For this, we selected the Topo to Raster function of ArcGIS, as it is often
233 considered to be one of the best methods for working with topographic data (Zheng et al., 2016). The
234 output cell size was set to 1 m, which is in good accordance with the accuracy of the initial data (grids
235 of 3 m), and did not lead to excessive interpolation. Previous studies showed that other interpolation
236 techniques (e.g. IDW, Kriging, EBK, RBFs) might also be suitable for deriving erosion surfaces (Rodrigo-
237 Comino et al., 2019), but an accurate evaluation of them was considered beyond this study. Volume
238 calculations (above and beyond the reference level - initial topsoil surface) were performed using the
239 3D analyst extension of ArcGIS to obtain the eroded and accumulated volume for each plot. The values
240 were aggregated at the plot scale and the erosion volume was subtracted from the accumulation
241 volume to obtain the net soil loss per plot. Finally, the values were reported relative to the surface

242 area (calculated using standard GIS tools), the age of vine (obtained from vine growers interview), and
 243 bulk density of the soil (measured in sampling cylinders – see section 3.1.4), to calculate a mean specific
 244 erosion rate expressed in $t \cdot ha^{-1} \cdot yr^{-1}$.



245

246 Figure 5: Location of the field investigations conducted

247 **3.1.4. Estimation of the error margin**

248 In the SUM method, five main types of error can influence the final soil loss results: (1) imprecision in
 249 the measurement of the space between the graft union and the ground; (2) variability of the distance
 250 between the ground and graft union when the vine stock is planted; (3) variations in the bulk density

251 of soils; (4) errors in the interpolation of the surface raster used for volumetric calculations; and (5)
252 the influence of the interrow morphology, as erosion tends to be more intense in the interrow than in
253 the vine row (Rodrigo-Comino and Cerdà, 2018). To integrate such margins of error, additional data
254 acquisitions were made.

255 To assess the direct effect of measurement error when a ruler is used, a set of 120 vine stocks were
256 subjected to repeat measurements after a 6-hour time interval. Additionally, we took the opportunity
257 to measure the distance between ground and graft union for a set of 99 vine stocks recently planted
258 in a new vineyard within the study area. The main objective was to assess the accuracy of the distance
259 from the graft union to the soil during vine stock planting. From these two sets of measurements, we
260 used a standard error calculation to determine the 95% confidence interval according to the following
261 formula (Altman and Bland, 2005):

$$262 \quad e = 1.96 \sqrt{\frac{\sigma}{n}}$$

263 where e is the confidence interval, 1.96 is a constant value obtained from the normal distribution table,
264 σ is the standard deviation, and n is the sample size.

265 Considering independence and additivity principles on the error values, the planting error and the
266 measurement error were combined using the quadratic sums of the individual terms.

$$267 \quad e_{total} = \sqrt{e_{planting}^2 + e_{measure}^2}$$

268 A set of 12 samples were collected in the field using calibrated cylinders to measure the bulk density
269 of the topsoil layer under different conditions. The two main types of soil were both sampled (four
270 samples each), and additional samplings were performed on materials recently extracted from a
271 sediment trap (Fig. 5). Mass calculations (volume \times bulk unit weight) were performed for every plot
272 using the minimum, maximum, and mean bulk density values, and these were added to the error
273 margin extent.

274 Two test rows of vines were measured using the ISUM method. These rows were in two distinct plots
275 characterized by contrasting agricultural practices: the presence or absence of ridging and un-ridging.
276 During the field survey, two distinct types of vine row morphology (V-shaped and flat) were observed,
277 and these were considered to be relevant to the investigation. We therefore conducted ISUM₅
278 measurements, which involved three additional points of measurements in the interrow. This resulted
279 in a total of five points: two graft union measurements, one on either side, and three measurements
280 in the interrow spaced at 25 cm, as the interrow length was 1 m. Higher resolution measurements
281 were not considered, as comparative studies showed that a five-point ISUM is a good compromise
282 between accuracy and the time required for field work (Rodrigo-Comino et al., 2019).

283 **3.2. Volume estimation in sediment traps**

284 The dredging of a sediment trap, a counter dip path, and a storm basin, offered the possibility to
285 measure trapped volumes in four main points of the study area. The volumes were estimated by
286 measuring the length, width, and height of earth mounds, and considering their shape as being
287 pyramidal. The measured volumes were then related to the bulk unit weight, the last dredging date
288 (obtained from the winegrowers association), and the upslope contributing area, to obtain the specific
289 accumulation rate in the sediment collector/path. The values are expressed in $t \cdot ha^{-1} \cdot yr^{-1}$. We arbitrarily
290 assumed a 10% error margin on the measurements made using this technique, which was added to
291 the variability in the bulk unit weights obtained from laboratory analyses.

292 **3.3. Comparing erosion rates with explanatory factors**

293 To feed the discussion on potential driving factors of soil erosion, several available terrain parameters
294 potentially contributing to soil erosion rates were compared to the measured values. The comparison
295 was provided at the plot scale, based on a pairwise qualitative evaluation of the relationship between
296 the driving factor and the measured erosion rates.

297 Slope angle was extracted from available Lidar DEM (1 m resolution) and plot length was calculated
298 using standard GIS tools. The USLE LS factor (Wischmeier and Smith, 1978) was derived for each plot

299 using the mean slope angle and slope length using the Renard et al. (1997) equations. L factor can be
300 represented as:

$$301 \quad L = \left(\frac{\lambda}{22.13} \right)^m$$

302 where λ is the slope length (in meters) and m is equivalent to 0.5 for slopes steeper than 5%, 0.4 for
303 slopes between 3%–4%, 0.3 for slopes between 1%–3% and 0.2 for slopes less than 1%.

304 The S factor can be represented as :

$$305 \quad S = 10.8 \times \sin \theta, \text{ where slope gradient} < 0.09$$

$$306 \quad S = 16.8 \times \sin \theta, \text{ where slope gradient} \geq 0.09$$

307 where θ is the gradient of slope in radians.

308 Soil surface stoniness and soil type were derived from the available soil map and validated by field
309 survey. The age of vine plots was also compared to the erosion rates as it has already been observed
310 as a controlling factor of soil erosion rates in previous studies (Casali et al., 2009 ; Rodrigo-Comino et
311 al., 2018a).

312

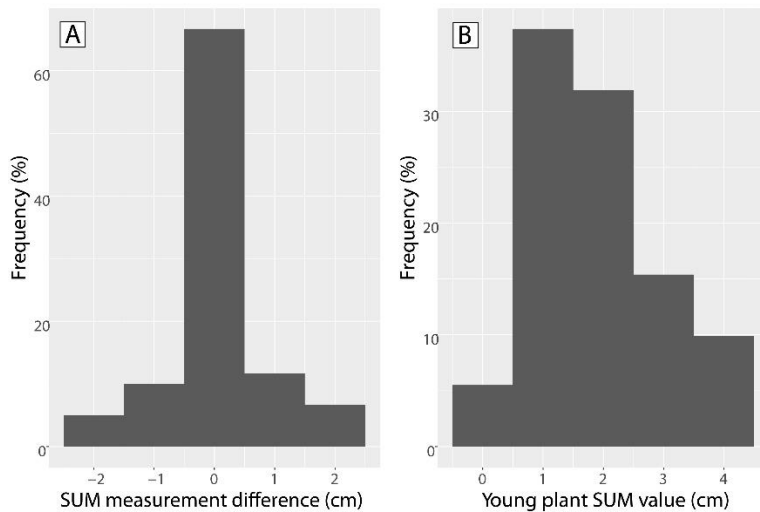
313 **4. Results**

314 **4.1. Methods implementation for erosion assessment**

315 **4.1.1. Measurements and volume calculations**

316 On the recently planted vineyard (<1 year-old) the mean measured plantation distance from the graft
317 union to the ground was found to be 1.87 cm, with a standard deviation of 1.07 cm (Fig. 6). This
318 returned a standard error of 0.11 and an error margin (accuracy of the mean) of 0.22. In addition, the
319 SUM measurements repeated on the same stocks after a 6-hour interval returned a perfect match for
320 66% of measurements, with another 21.6% being within 1 cm. The final calculated error margin of the

321 measurement was 0.21 cm. Combining these two error margins returned a mean error of 0.33 cm per
322 vine plant. Therefore, the volume calculations are systematically processed within this range (mean \pm
323 0.33 cm).

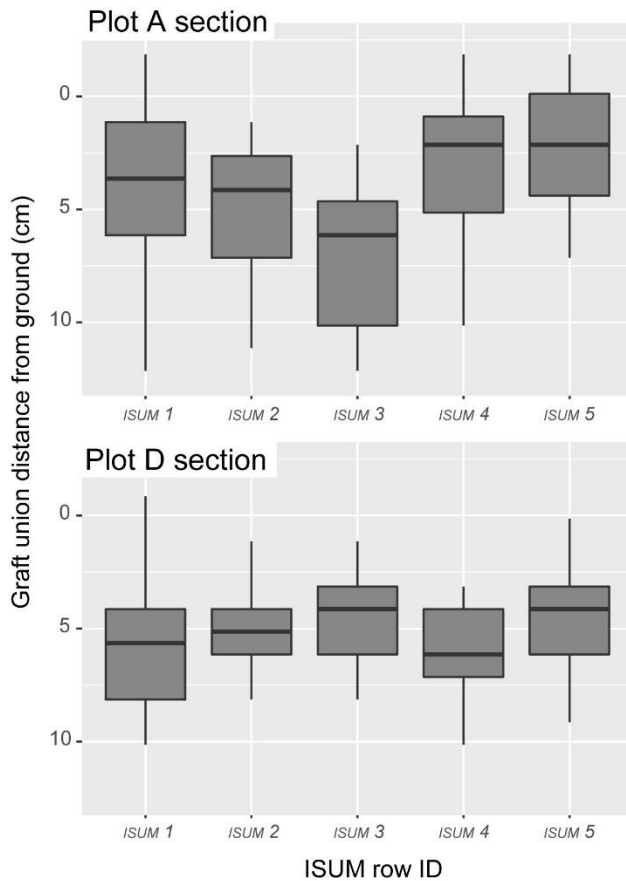


324
325 Figure 6: Distributions of the accuracy assessments of SUM difference (A) and measurement of young
326 plants (B).

327 On plot B, the mean bulk density was 16.5 KN/m³ (values ranged from 15.6 to 17.2), whereas on plot
328 D it was 15.38 KN/m³ (values ranged from 15.7 to 15.9). The bulk density of the material in the
329 sediment trap was 13.8 KN/m³ (values ranged from 13.6 to 14.3), and was lower because of the
330 decompression of sediments due to transport and the absence of compaction by tractors. The
331 conversion of eroded volumes to mass was therefore performed within the range of these measured
332 values (mean, maximum, and minimum).

333 **4.1.2. ISUM correction**

334 The two test vine plots showed a variety of interrow conditions and morphology, which resulted in
335 diverse ISUM correction factors. The ISUM section of plot A (Fig. 7) clearly shows a general V-shaped
336 interrow morphology, which is contrary to the ISUM section of plot D, which shows a planar section
337 between the row and interrow (Fig. 7).



338

339 Figure 7: Boxplots of ISUM distribution over the two cross sections measured on plot A and plot D.

340 Reported to the initial top-soil level, vine row length, and width, the estimated erosion rates on these
 341 two cross sections were 10.6 and 17.3 t.ha⁻¹.yr⁻¹ for section A using SUM and ISUM, respectively, and
 342 58.2 and 58.3 t.ha⁻¹.yr⁻¹ for section D. These results indicate two main correction factors that can be
 343 applied in regards to the interrow morphology. First, a correction factor of 40% can be considered in
 344 the case of V-shaped interrows similar to those in plot A. Contrastingly, no correction factor need be
 345 applied on plots characterized by a flat morphology (no deep incision affecting the interrow). Finally
 346 on the basis of these field observations, a 40% ISUM correction factor was applied to results from plot
 347 A, B, and F, whereas results from plots C, D, E, and G were not corrected.

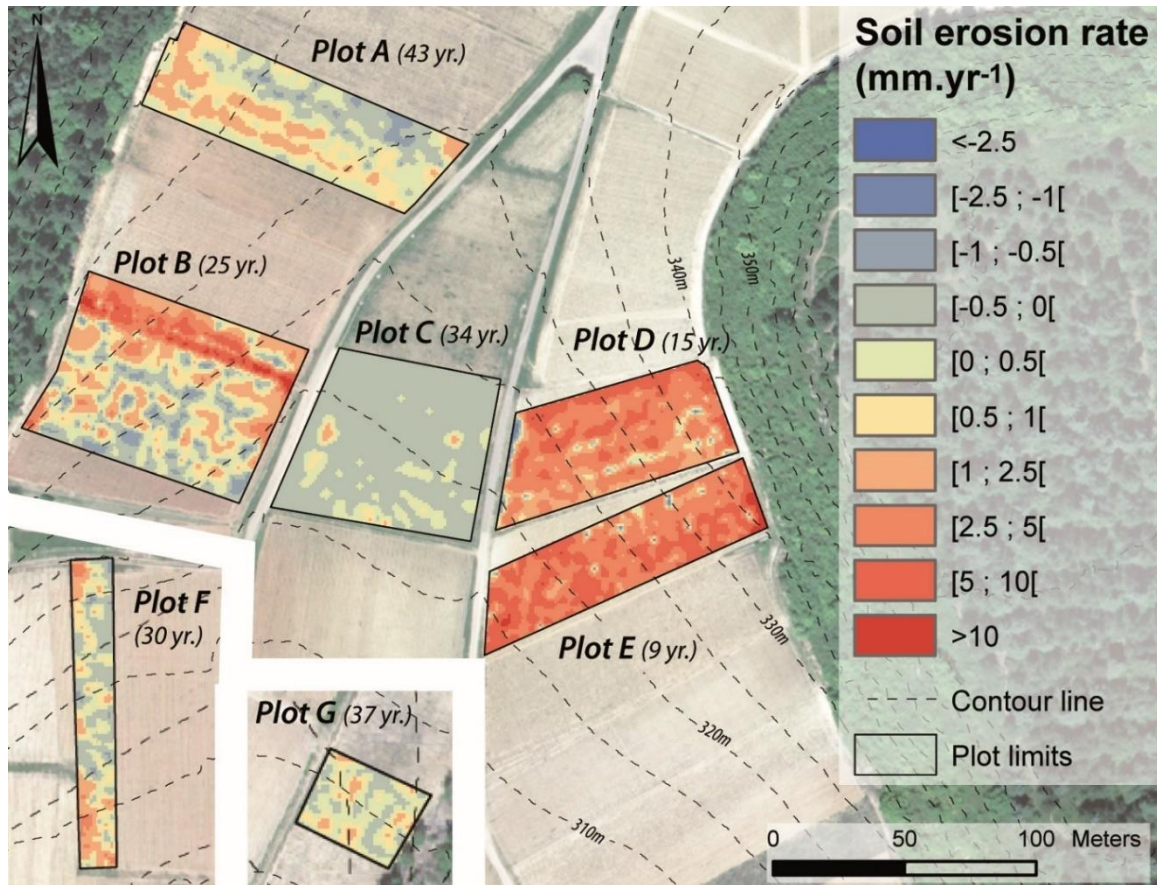
348

4.2. Soil erosion rates at the plot scale

349 The mean soil loss measured on the seven plots was 21.4 ± 3.1 t.ha⁻¹.yr⁻¹. This average hides a wide
 350 diversity of local situations (Figs. 8 and 9, Table 1). Plot A is characterized by a mean erosion rate of 10

351 $\pm 2.2 \text{ t}\cdot\text{ha}^{-1}\cdot\text{yr}^{-1}$, which corresponds to a mean ablation of $0.5 \pm 0.1 \text{ mm}\cdot\text{yr}^{-1}$ over a measured timescale
352 of 43 years. The mean slope gradient is 6.9° , the slope length is 118 m, LS factor is 3.5 and soil surface
353 stoniness is between 35 to 40%. This plot shows higher erosion rates on the upslope part (south west)
354 associated with a slight increase in slope gradient. Plot B has a mean erosion rate of $32.1 \pm 4.5 \text{ t}\cdot\text{ha}^{-1}\cdot\text{yr}^{-1}$
355 ($1.5 \pm 0.1 \text{ mm}\cdot\text{yr}^{-1}$). The mean slope is 10.2° , the plot length 89 m, LS factor is 5 and stoniness is
356 between 35 to 40%. This plot is characterized by the presence of a small gully ($\pm 30/40 \text{ cm}$ deep and 1
357 m wide) on its north side, which significantly increases its mean erosion. It is developed on four vine
358 rows on top, which converge together to form one unique row downslope. With the exclusion of the
359 gully, the plot erosion rate drops to $15.8 \pm 3.6 \text{ t}\cdot\text{ha}^{-1}\cdot\text{yr}^{-1}$, while the gully itself represents a mean erosion
360 rate of $81.1 \pm 5.7 \text{ t}\cdot\text{ha}^{-1}\cdot\text{yr}^{-1}$. Field observations showed that this gully originates from a dysfunction in
361 the sediment collection system. A small local breach in the counter dip path creates an overspill of the
362 accumulated flow directly into the plot, which drastically increases local runoff. Plot C is characterized
363 by aggradation, as the measured erosion rate was $-3.2 \pm 1.5 \text{ t}\cdot\text{ha}^{-1}\cdot\text{yr}^{-1}$ ($-0.2 \pm 0.1 \text{ mm}\cdot\text{yr}^{-1}$). The mean
364 slope is 6.6° (the lowest gradient of all the slopes, but close to that of plot A), the length 77 m, LS factor
365 is 2.7 and stoniness is between 30 to 35%. According to information obtained from interviews with the
366 vine growers, this plot was recently backfilled (5 years ago), potentially contributing to its significant
367 aggradation. Moreover, this plot is characterized by the lowest LS factor of the selected plots
368 constituting also a context potentially less favorable to erosion. Plots D and E are affected by severe
369 erosion rates of $43.1 \pm 3.6 \text{ t}\cdot\text{ha}^{-1}\cdot\text{yr}^{-1}$ ($3.5 \pm 0.2 \text{ mm}\cdot\text{yr}^{-1}$) and $53 \pm 5.8 \text{ t}\cdot\text{ha}^{-1}\cdot\text{yr}^{-1}$ ($4.7 \pm 0.4 \text{ mm}\cdot\text{yr}^{-1}$),
370 respectively. These two plots have the highest LS factor (respectively 6.4 and 6.5), have a high stoniness
371 (45 to 50%) and are the youngest measured in this study (15 and 9 years, respectively). The maps show
372 a very regular pattern of erosion at the plot scale. Plot F was affected by an erosion rate of 10 ± 2.8
373 $\text{t}\cdot\text{ha}^{-1}\cdot\text{yr}^{-1}$ ($0.5 \pm 0.1 \text{ mm}\cdot\text{yr}^{-1}$) over a timescale of 30 years. The mean slope is 9.1° , the plot length is 100
374 m, LS factor is 4.6 and stoniness is between 30 and 35%. The downslope part of the plot is slightly more
375 affected by erosion than the upslope part. Plot G was affected by soil erosion of $4.6 \pm 1.3 \text{ t}\cdot\text{ha}^{-1}\cdot\text{yr}^{-1}$ (0.3
376 $\pm 0.1 \text{ mm}\cdot\text{yr}^{-1}$) over 37 years. The mean slope is 17.7° , the plot length 27 m. This plot is characterized

377 by a high LS factor of 5.1 (especially influenced by slope steepness while slope length is low) and a high
 378 stoniness (55 to 60%). Despite its steep slope and the absence of collecting infrastructure upslope (no
 379 counter dip path), this old vineyard is affected by a lower erosion rate than the other steep slopes
 380 plots.



381
 382 Figure 8: Erosion maps of the seven plots investigated

383

384 4.3. Comparison with potential driving factors

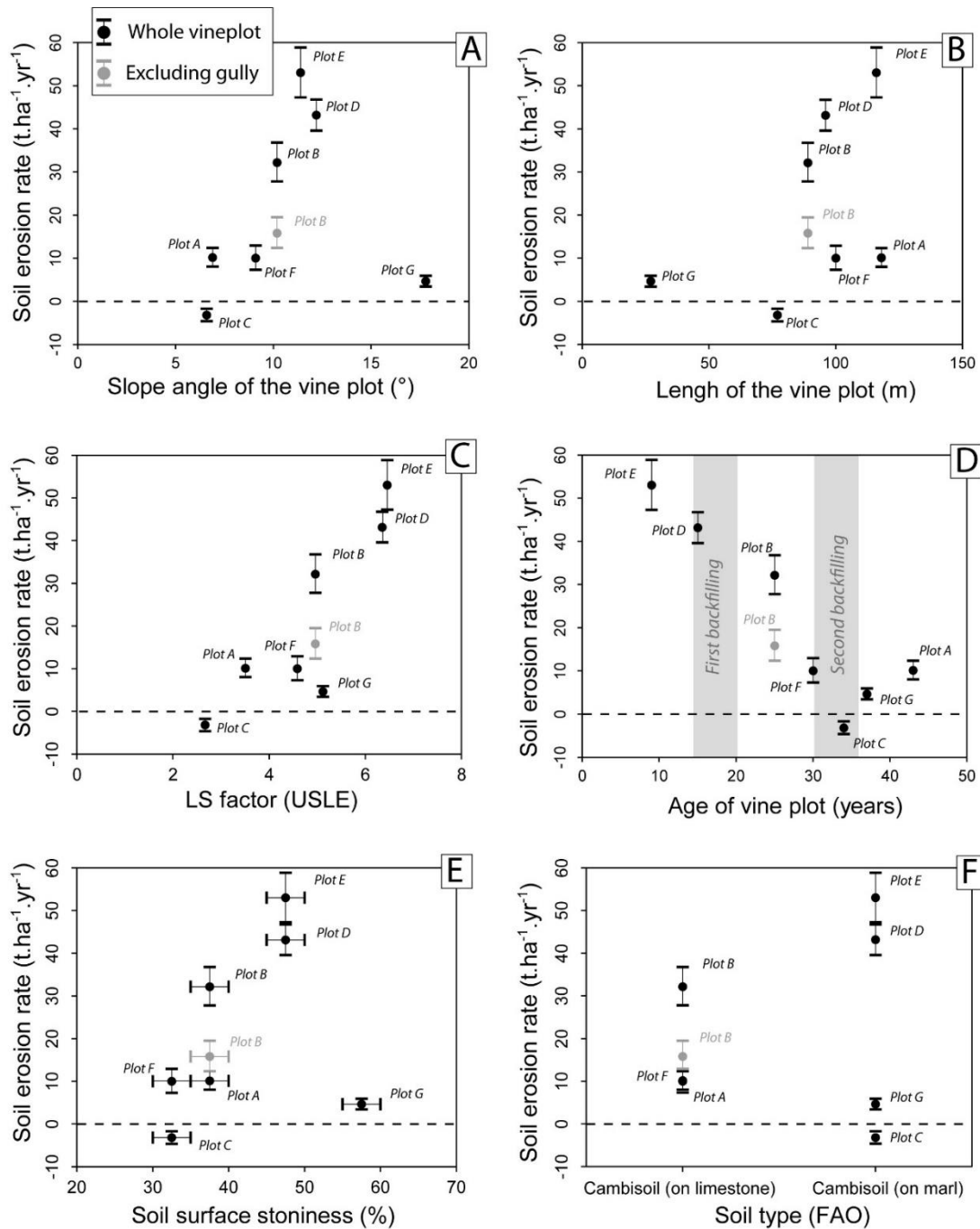
385 Unsurprisingly, we can notice an apparent link between topography and the soil erosion rate (fig. 9-A,
 386 B and C). Especially observing the correlation with the USLE LS factor ($R^2 = 0.72$). Plots characterized
 387 by low LS factors systematically show lower erosion: plots C and A exhibit LS factors below 4 and
 388 erosion rates below $10 \text{ t.ha}^{-1}.\text{yr}^{-1}$. On the opposite plots D and E exhibit high LS factor (above 6) and

389 high erosion rates, above $40 \text{ t}\cdot\text{ha}^{-1}\cdot\text{yr}^{-1}$. Plot G tends to be affected by a soil erosion lower than expected
390 since in spite of a high LS factor (5.1) shows moderate soil erosion rate $4.6 \pm 1.3 \text{ t}\cdot\text{ha}^{-1}\cdot\text{yr}^{-1}$.

391 Comparing the age of vines with soil erosion rates also shows a good correlation (Fig. 9-D, $R^2 = 0.79$).
392 The two “young” (i.e., less than 15 years) vine plots (D and E) showed very high erosion rates above 40
393 $\text{t}\cdot\text{ha}^{-1}\cdot\text{yr}^{-1}$. Plot B, which is of an intermediate age (25 years), is characterized by a high to intermediate
394 erosion rate of $15.8 \pm 3.6 \text{ t}\cdot\text{ha}^{-1}\cdot\text{yr}^{-1}$ (excluding the gully), while the other vine plots (more than 30 years
395 old) tend to show lower values (less than $10 \text{ t}\cdot\text{ha}^{-1}\cdot\text{yr}^{-1}$) or aggradation (plot C).

396 A relationship can be visually deduced between soil surface stoniness and soil erosion rates (even if R^2
397 is low: 0.11, fig. 9.E). Plots affected by higher erosion rates are characterized by a higher surface
398 stoniness. This relationship appears counterintuitive since the soil surface stoniness is often
399 considered having a negative effect on sediment yield and thus, can be considered as natural soil-
400 surface stabilizer (e.g. Poesen and Ingelmo-Sánchez, 1992). In this case, it can be interpreted as a
401 preferential export of fine sediments by runoff, increasing the coarse material fraction on plots
402 affected by severe erosion. Only plot G can be seen as an exception in this case, which can be explained
403 by the backfilling or by the proximity of the plateau edge which can efficiently feed soil surface with
404 coarse elements.

405 No clear trend can be observed between the soil types and erosion rates as the plots appears unevenly
406 distributed on fig. 9-F. This could be explained by homogeneity of soil types on the study area: both
407 types of soils are Cambic calcic soils, which are only distinguished by the parent material marls and
408 marly-limestone.



409

410 Figure 9: Measured erosion rates according to some explanatory factors. (A) slope angle, (B) slope

411 length, (C) USLE-LS factor, (D) age of vines, (E) soil surface stoniness and (F) soil type.

412

413

414

415

4.4. Sub-catchment scale sediment transfer and connectivity

416

In the intermediate counter slope created by a transverse track, the trapped volume of sediments was

417

quantified to be $30 \pm 3 \text{ m}^3$ for a drained surface of 2.24 ha. These counter slopes are regularly dredged

418

(every 1 to 2 years), depending on their filling rate. We measured the potential erosion over the period

419

of a year to be $16.6 \pm 5.9 \text{ t}\cdot\text{ha}^{-1}\cdot\text{yr}^{-1}$, which is of a comparable order of magnitude to the mean erosion

420

measured on the parcels. On the two sediment traps located downslope of the catchment, the

421

investigations performed by Fressard et al. (2019) allowed evaluation of an erosion rate of 1.31 ± 0.7

422

$\text{t}\cdot\text{ha}^{-1}\cdot\text{yr}^{-1}$ for trap one. A value of $0.15 \pm 0.05 \text{ t}\cdot\text{ha}^{-1}\cdot\text{yr}^{-1}$ was assessed for the second trap, but this was

423

affected by construction problems limiting its connectivity to the vine plots and its drainage efficiency.

424

Finally, the sediment export rate measured in a storm basin connected to the main river of the

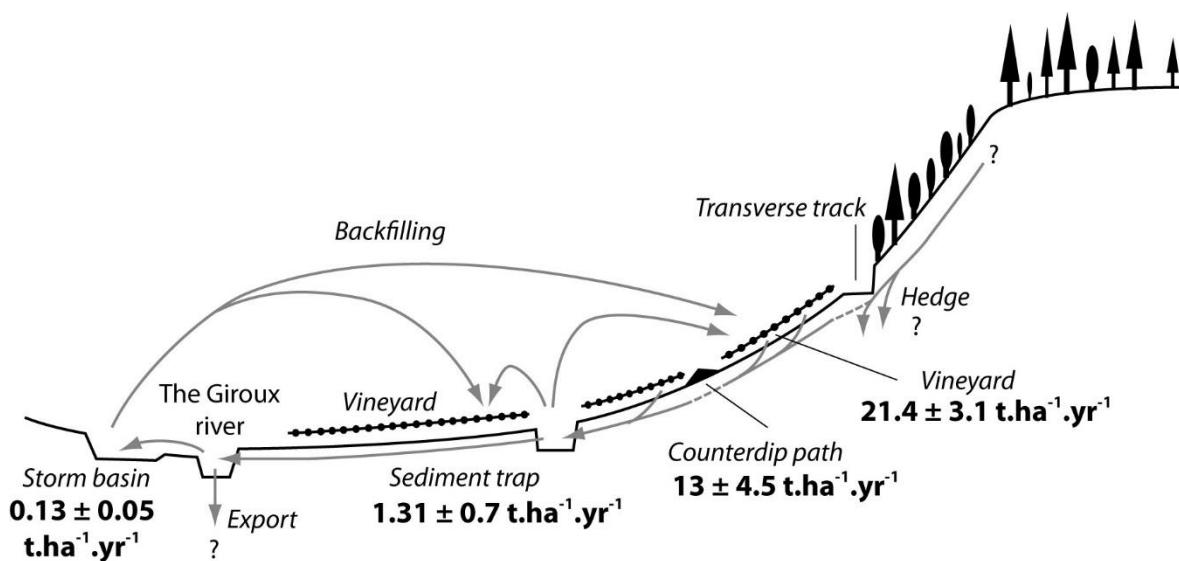
425

catchment provided a result of $0.13 \pm 0.05 \text{ t}\cdot\text{ha}^{-1}\cdot\text{yr}^{-1}$, which is much lower than the erosion rates

426

measured on the vine plots, and the sediment traps and counter dip path of the upper slopes.

427



428

Figure 10: Sediment cascade in the Mercurey vineyards

429

430

From a general point of view, the specific erosion rates tend to decrease closer to the catchment outlet

431

(Fig. 10). This observation is frequent in geomorphology, and it can be explained here by the effect of

432 landscape rugosity, the presence of anthropogenic counter slopes and traps, and the progressive
 433 decrease in slope gradient moving down the catchment. The contributing areas of the sediment traps
 434 and storm basin are wide (several hectares), favoring multiple intermediate sediment storage areas.
 435 This assumption can be easily confirmed in the field after intense storms, where numerous small
 436 sediment accumulations can be observed in various areas of the catchment (e.g., slope breaks between
 437 vine plots and roads, small ditches, counter slopes, Fig. 11).

438

439 Table 1: Erosion rates at the plot scale

Plot	Age / timescale (yrs)	Area (ha)	Bulk unit weight (KN/m ³)	ISUM correcti on factor	Mean slope angle (°)	Slope length (m)	Surface lowering (mm.yr ⁻¹)	Exported volume (m ³)	Exported mass (t.)	Soil loss (t.ha ⁻¹ .yr ⁻¹)
A	43	0.41	16.5 ± 0.8	0.4	6.9	118	0.5 ± 0.1	77 ± 12.8	127.1 ± 27.3	10.1 ± 2.2
B	25	0.57	16.5 ± 0.8	0.4	10.2	89	1.5 ± 0.1	199.9 ± 18.3	329.9 ± 46.1	32.1 ± 4.5
<i>B (gully area)</i>	25	0.07	16.5 ± 0.8	0	10.2	89	6.2 ± 0.1	86 ± 1.8	142 ± 9.9	81.1 ± 5.7
<i>B (ex. gully)</i>	25	0.52	16.5 ± 0.8	0.4	10.2	89	0.8 ± 0.1	88.9 ± 15.7	146.7 ± 33	15.8 ± 3.6
C	34	0.46	15.8 ± 0.1	0	6.6	77	-0.2 ± 0.1	-31.7 ± 14.6	-50 ± 22.8	-3.2 ± 1.5
D	15	0.35	15.8 ± 0.1	0	12.2	96	3.5 ± 0.2	143.4 ± 11	226.5 ± 18.9	43.1 ± 3.6
E	9	0.33	15.8 ± 0.1	0	11.4	116	4.7 ± 0.4	98.6 ± 10.2	155.9 ± 17	53 ± 5.8
F	30	0.13	16.5 ± 0.8	0.4	9.1	100	0.5 ± 0.1	12.9 ± 3.9	27.8 ± 7.8	10 ± 2.8
G	37	0.06	15.8 ± 0.1	0	17.8	27	0.3 ± 0.1	4.5 ± 1.6	9.5 ± 2.6	4.6 ± 1.3
Counter dip path	1	2.50	13.8 ± 0.35	x	x	x	x	30 ± 3	41.4 ± 14.6	16.6 ± 5.9
S. trap 1	4	17.10	13.8 ± 0.35	x	x	x	x	65 ± 6.5	89.7 ± 31.7	1.31 ± 0.7
S. trap 2	28	16.50	13.8 ± 0.35	x	x	x	x	50 ± 5	69 ± 24.4	0.15 ± 0.05
Storm basin	28	300	13.8 ± 0.35	x	x	x	x	800 ± 80	1104 ± 390	0.13 ± 0.05

440

441



442

443 Figure 11: Deposition patterns observed in the field (A) deposition downslope a vine plot following a
 444 main runoff axis, (B) deposition in a ditch and (C) recently dredged deposition area on the downslope
 445 break of a vine plot

446 **5. Discussion**

447 **5.1. Erosion rates and drivers observed in other vineyards using SUM and ISUM**

448 Other studies have used the SUM technique to measure and map soil erosion at the plot scale. Globally,
 449 our measurements are consistent with those of Brenot et al. (2006, 2008), who measured values in
 450 Vosne-Romanée, Aloxe-Corton, and Monthélie ranging from 7.6 to 23 t.ha⁻¹.yr⁻¹ over timescales from
 451 32 to 54 years. Brenot (2007) found a relationship between local topography (slope angle) and the
 452 level of soil erosion for slopes inferior to 10°. When slopes exceed this threshold, erosion rates appear
 453 to be function of the upslope area. Chevigny et al. (2014) have highlighted the role of historical

454 landscape structures (such as dry-stone walls) in the case of low erosion. In the case of severe erosion,
455 geomorphological drivers especially slope) dominate (runoff). Still in Burgundy, Quiquerez et al. (2014)
456 compared SUM measurements with DEMs and high resolution mapping of soil surface stoniness. Both
457 factors were found to be influential: higher erosion rates were observed on steeper slopes, while high
458 surface stoniness tends to reduce the erosion susceptibility. Rodrigo-Comino et al. (2017) directly
459 measured the effect of vineyard age on erosion and found a value of $62.5 \text{ t}\cdot\text{ha}^{-1}\cdot\text{yr}^{-1}$ for young vineyards
460 compared with $3.3 \text{ t}\cdot\text{ha}^{-1}\cdot\text{yr}^{-1}$ for old ones. A similar pattern was later confirmed by Rodrigo-Comino et
461 al. (2018a), ranging from $8.2 \text{ t}\cdot\text{ha}^{-1}\cdot\text{yr}^{-1}$ for young vineyards (2 years old) to $1.6 \text{ t}\cdot\text{ha}^{-1}\cdot\text{yr}^{-1}$ for old ones
462 (25 years). In these studies, the authors interpreted that most of the increase in the distance between
463 graft union and ground happens during the early years after plantation since unconsolidated soils are
464 more prone to erosion and compaction. Then, erosion rates get stabilized since compaction leads to a
465 lower sensitivity of soils. The same trend was observed by Casali et al. (2009) in Spain, with values of
466 36 to $50 \text{ t}\cdot\text{ha}^{-1}\cdot\text{yr}^{-1}$ for young plots versus 14 to $20 \text{ t}\cdot\text{ha}^{-1}\cdot\text{yr}^{-1}$ for older ones. In this study, the absence
467 of correlation between slope and erosion level was interpreted as a major role played by tillage erosion
468 that is sometimes considered among the most important driving factor of soil loss in agricultural lands
469 (e.g. Govers et al., 1999). Paroissien et al. (2010) measured a mean erosion of $10.5 \text{ t}\cdot\text{ha}^{-1}\cdot\text{yr}^{-1}$ in
470 Languedoc, with individual values ranging between -27.5 to $66.7 \text{ t}\cdot\text{ha}^{-1}\cdot\text{yr}^{-1}$. They found that slope
471 angle and the degree of connectivity (presence or absence of obstacles to runoff on the upslope of the
472 vine plot) showed direct relationships with the intensity of soil erosion.

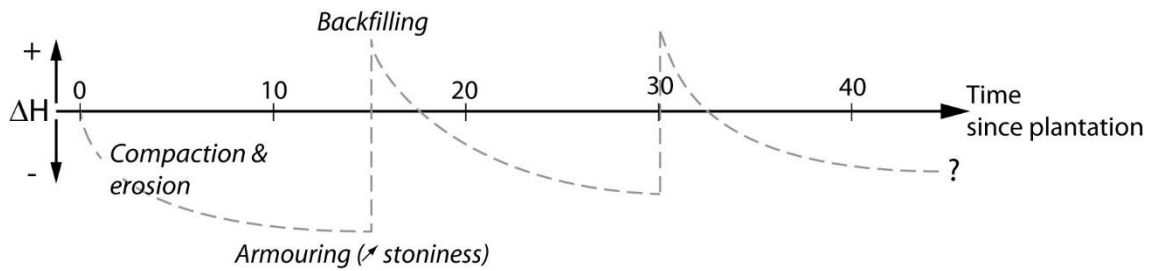
473

474 **5.2. The driving factors of erosion in Mercurey**

475 In the case of Mercurey, it can be stated that runoff plays a significant part in the erosion process, as
476 attested by several rill/gully shapes, fans downslope the plots and a good correlation between erosion
477 rates and USLE-LS factor. The regular (but not systematic) observation of a high degree of stoniness on
478 highly eroded slopes is a supplementary indicator of ongoing sheet wash erosion processes.

479 In addition, the specific practice that consists in backfilling eroded plots with collected soils should be
480 accounted for in the sediment budget to explain the variations of erosion rates regarding the age of
481 vines. This practice reveals a cyclicity in ground elevation variability within vine parcels, as documented
482 by local vine growers. Three steps may be exhibited. First, terraced and deeply-tilled soils combined
483 with low vegetation cover (young plants) are more sensitive to splash and runoff. In addition, tractor
484 compaction is potentially very efficient on these still uncompacted soils: compaction rates (based on
485 bulk density) ranging from 10% to 20% are often observed in various physical and anthropogenic
486 settings (van Dijck and van Asch, 2002 ; Elaoud and Chehaibi, 2011 ; Botta et al., 2012). Although it
487 remains difficult to assess the respective parts of erosion and compaction using the SUM/ISUM
488 method, a rapid increase in the distance between the graft union and the soil is clear over the first
489 years after plantation, and its measurement therefore integrates both processes. Local vine growers
490 estimate that the stage of compaction generally lasts for 3 to 5 years (Fig. 12). After a period of 10 to
491 15 years, the plots show a significant decrease in erosion rate. A progressive reduction of soil erodibility
492 does indeed occur in relation to soil compaction and progressive armoring of soils: erodible loamy soil
493 particles are progressively exported and their stocks become exhausted. Then, soil surface stoniness
494 increases.

495 Consequently, anthropogenic backfilling is performed. In Burgundy, vine-growers apply this strategy
496 every 15 to 20 years, depending on the local situation. In the case of extreme morphogenic hydro-
497 meteorological events, backfilling may occur more frequently. The objective of backfilling is to
498 compensate for soil losses by adding an external supply of soil, providing earth material to cover the
499 graft-union. Therefore, in old vineyards, the measured erosion rates (considering the time elapsed
500 since plantation) may reveal an apparent equilibrium. The results obtained on the oldest vineyards in
501 Mercurey (plots A and G) do indeed show that the erosion rates stabilized at between roughly 4.5 to
502 10 t.ha⁻¹.yr⁻¹ over long time periods (many decades). However, these values remain much higher than
503 the estimated tolerable erosion rates for sustainable development of agriculture (Verheijen et al.,
504 2009).



505

506 Figure 12: Cyclicity in ground elevation in vine parcels. The succession of three main stages is exhibited:
 507 compaction, armorings, and backfilling.

508

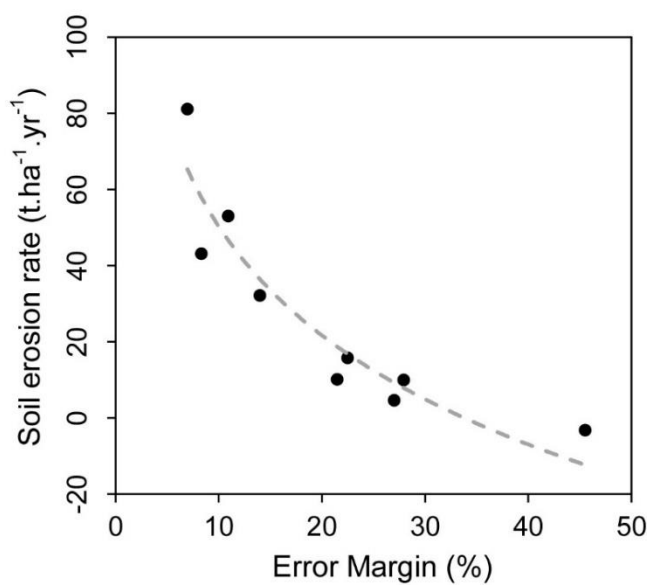
509 On the one hand, anthropogenic backfilling can appear to be an efficient strategy to cope with soil
 510 losses, but on the other hand, it can also be considered a resetting of sediment sources. Recent
 511 observations of flash floods following intense rainstorms revealed high concentrations of suspended
 512 particles, suggesting that vine parcels remain a significant source of sediments. Large amounts of fine
 513 particles are still supplied and exported from the catchment, despite the sediment trapping system.
 514 Further research is needed to accurately estimate the efficiency of trapping systems, especially on fine-
 515 size particles.

516

517 **5.1. Methodological feedback and error margins**

518 In this study, the estimated cumulative error margins associated with (1) manual measurement of the
 519 height, (2) vine plantation accuracy, and (3) soil bulk unit weight estimation are variable (from 7% to
 520 45% of the final estimated value in $t \cdot ha^{-1} \cdot yr^{-1}$). The error margin is a direct function of the intensity of
 521 observed erosion, and tends to be less influential in the case of high-level erosion (fig. 13). Then, more
 522 than the age of vines, the level of erosion is the most influential factor on the error. Therefore, the
 523 measurements of plots affected by erosion rates of less than $10 t \cdot ha^{-1} \cdot yr^{-1}$ must be interpreted with
 524 caution as the error margin might exceed 25%. Nevertheless, the approach still allows provision of the
 525 overall order of magnitude of the intensity of erosion, even if lower erosion rates are affected by more

526 uncertainty. The studies of Brenot et al. (2008), Chevigny et al. (2014) and Quiquerez et al. (2014)
527 explicitly expressed the final estimated erosion rate within the error margin range and allow
528 comparison. In these articles, error margins that includes plantation, measurement errors and bulk
529 unit weight were found to be between 20 to 40%. Other studies (e.g. Casalí et al., 2009 ; Paroissien et
530 al., 2010 ; Rodrigo-Comino et al., 2016) also assessed the error. They conclude that in spite of the error
531 margin the method is still applicable, given that the overall soil loss is much higher than the
532 experimental error.



533

534 Figure 13: Relationship between the soil erosion rate and error margin

535

536 The repeatability of a vine stock measurement in the field is among the factors that tends to increase
537 the error margins. This error is mostly due surface roughness and stoniness that can make the graft
538 union height measurement difficult. We applied standardized techniques already published to make
539 comparison easier (Brenot et al., 2008; Paroissien et al., 2010). The imprecisions of the graft union
540 height at plantation is also a source of uncertainty that can not be avoided. The measurement of a
541 control plot (recently planted vineyard) allowed estimating a standard deviation of 1.07 cm (standard
542 error 0.22) which is in good agreement with findings of Brenot et al. (2006, 2008) and Paroissien et al.

543 (2010) who found a value of 1 cm. Casalí et al. (2009) found a value of 2 cm. Bulk unit weight is also a
544 source of variability in the final conversion of the results from volume to mass that is not systematically
545 measured (this parameter is often deduced from bibliographic review and set between 12.5 to 15
546 KN/m³). In our study, we used a total of 12 samples for bulk unit weight calculations separated in 2
547 types of soils and sediments accumulated in traps. The use of more points of control (several
548 measurements per plot at different depth) may improve slightly the estimate of erosion.

549 The ISUM correction factor, which was first applied to Spanish vineyards by Rodrigo-Comino and Cerdà
550 (2018), was shown to be of relevance to our case study. However, the diversity of the interrow
551 morphologies also demonstrates that this technique should be applied with caution, and the
552 correction factor was differently applied according to the interrow morphology and field expertise. In
553 this case study, the ISUM correction value for three plots was 40%, which is much higher than the
554 25.7% proposed by Rodrigo-Comino and Cerdà (2018) for Spanish vineyards. However, four plots were
555 characterized by a correction factor of 0%. This approach is more accurate than the traditional SUM
556 method, but extends the data acquisition time in the field (between 1.5 to 2 times longer on the basis
557 of our experience). Therefore, it remains more difficult to deploy the ISUM method over large areas.
558 Our estimate of the ISUM correction factor is, in this case study, only based on two rows. A larger
559 application of the comparison and also higher resolution measurements in the interrow might help
560 increase the accuracy of the correction factor, which may vary from plot to plot, even on the same
561 catchment and with relatively similar agricultural practices.

562 The comparison of long-term soil erosion on vine plots with short-term measurements in sediment
563 traps and the counter dip path (i.e., 1 to 4 years) allowed a general assessment of the order of
564 magnitude of erosion, but this assessment still remains difficult. The short-term measurements may
565 be affected (positively or negatively) by the presence or absence of extreme events that may bias the
566 approach. In this sense, regular monitoring of sediment traps and other sediment sinks within the
567 catchment may be of great interest for detailing the sediment budget.

568 Finally, this method is based on the pluri-decennial assessment of the total exported volume and thus
569 integrates all anthropogenic actions that can be conducted on plots. Tractor compaction, tillage
570 erosion, backfilling and eventually application of organic fertilizers (rare in Burgundian vineyards) are
571 implicitly accounted when measuring the erosion rate. In that sense, comparing the measured erosion
572 rates with a detailed modelling might be a future perspective to assess the respective part of direct
573 anthropogenic actions and natural processes (runoff) within the observed erosion rate.

574

575 **6. Conclusions**

576 We used the SUM/ISUM measurement technique to estimate pluri-decennial soil erosion rates on
577 seven experimental plots in the Mercurey region of Burgundy. The mean erosion rate was 21.4 ± 3.1
578 $\text{t}\cdot\text{ha}^{-1}\cdot\text{yr}^{-1}$, but varied substantially from $-3.2 \pm 1.5 \text{ t}\cdot\text{ha}^{-1}\cdot\text{yr}^{-1}$ to $53 \pm 5.8 \text{ t}\cdot\text{ha}^{-1}\cdot\text{yr}^{-1}$. A variable ISUM
579 correction factor was applied, depending on the interrow morphology, which is directly influenced by
580 the vine growers' practices (e.g., the presence or absence of tillage and ridging/un-ridging of the vine
581 rows). The SUM/ISM was complemented by volumes measurements in sediment traps and in a counter
582 dip path. A decreasing trend of the specific erosion rate was observed along hillslopes (upslope to
583 downslope) (from 16.6 ± 5.9 in the most upstream counter dip path to 0.13 ± 0.05 in a storm basin
584 downstream). The results were complemented by an assessment of error margins, that are ranging
585 from 7% to 43%. Such values are directly correlated with the erosion rate: the higher the erosion rate,
586 the lower the error margin.

587 Hillslope erosion appears to be controlled by runoff (rill, inter-rill). Age-related differences in the level
588 of soil erosion has been observed and can originate from (1) the higher sensitivity of soil during the
589 first years after plantation (unconsolidated and bare soil), which tends to be reduced after a few years
590 (canopy development and tractor compaction); and (2) more specific to Burgundy, the regular (every
591 15 to 20 years) backfilling of eroded plots with soil collected in downslope sediment traps. Spatial
592 variability of erosion illustrates the effect of sediment connectivity and the efficiency of man-made

593 infrastructures to store eroded sediments from plots and hamper sediment transfer to rivers
594 (landscape rugosity, slope breaks between vine plots and roads, small ditches, counter slopes, sediment
595 traps, etc.). In addition, Despite this technique, the erosion rates remain high (especially on vine plots),
596 and suggest that backfilling from sediment traps should be combined with other soil erosion mitigation
597 techniques that maintain soils on plots (e.g., grass strips on the interrow, mulching), taking action on
598 the source area rather than managing its consequences.

599

600 **7. Acknowledgments**

601 We thank the winemakers association of Mercurey, especially Mr. Duvernay and Mr. Menand, for their
602 interest in our research and for sharing their practical field knowledge in constructive discussions. We
603 are grateful to the trainees Antoine Potot, Clément Alami, and Guillaume Brun for their help during
604 field surveys. This research was funded by the CNRS PEPS-INEE project DES-MES.

605 **8. References**

- 606 Altman, D.G., Bland, J.M., 2005. Standard deviations and standard errors. *British Medical Journal* 331,
607 903. <https://doi.org/10.1136/bmj.331.7521.903>
- 608 Arnaez, J., Lasanta, T., Ruiz-Flaño, P., Ortigosa, L., 2007. Factors affecting runoff and erosion under
609 simulated rainfall in Mediterranean vineyards. *Soil and Tillage Research* 93, 324–334.
610 <https://doi.org/10.1016/j.still.2006.05.013>
- 611 Battany, M.C., Grismer, M.E., 2000. Rainfall runoff and erosion in Napa Valley vineyards: effects of
612 slope, cover and surface roughness. *Hydrological Processes* 14, 1289–1304.
613 <https://doi.org/10/bskpd2>
- 614 Biddoccu, M., Ferraris, S., Opsi, F., Cavallo, E., 2016. Long-term monitoring of soil management effects
615 on runoff and soil erosion in sloping vineyards in Alto Monferrato (North–West Italy). *Soil and*
616 *Tillage Research* 155, 176–189. <https://doi.org/10.1016/j.still.2015.07.005>

617 Boardman, J., 2006. Soil erosion science: Reflections on the limitations of current approaches. *CATENA*,
618 Soil Erosion Research in Europe 68, 73–86. <https://doi.org/10.1016/j.catena.2006.03.007>

619 Botta, G.F., Tolon-Becerra, A., Tourn, M., Lastra-Bravo, X., Rivero, D., 2012. Agricultural traffic: Motion
620 resistance and soil compaction in relation to tractor design and different soil conditions. *Soil
621 and Tillage Research* 120, 92–98. <https://doi.org/10/b4m7nf>

622 Brenot, J., 2007. Quantification de la dynamique sédimentaire en contexte anthropisé. L'érosion des
623 versants viticoles de Côte d'Or. PhD Thesis, Université de Bourgogne.

624 Brenot, J., Quiquerez, A., Petit, C., Garcia, J.-P., 2008a. Erosion rates and sediment budgets in vineyards
625 at 1-m resolution based on stock unearthing (Burgundy, France). *Geomorphology* 100, 345–
626 355.

627 Brenot, J., Quiquerez, A., Petit, C., Garcia, J.-P., 2008b. Erosion rates and sediment budgets in vineyards
628 at 1-m resolution based on stock unearthing (Burgundy, France). *Geomorphology* 100, 345–
629 355. <https://doi.org/10.1016/j.geomorph.2008.01.005>

630 Casalí, J., Giménez, R., De Santisteban, L., Álvarez-Mozos, J., Mena, J., de Lersundi, J.D.V., 2009.
631 Determination of long-term erosion rates in vineyards of Navarre (Spain) using botanical
632 benchmarks. *Catena* 78, 12–19. <https://doi.org/10.1016/j.catena.2009.02.015>

633 Casalí, J., Loizu, J., Campo, M.A., De Santisteban, L.M., Álvarez-Mozos, J., 2006. Accuracy of methods
634 for field assessment of rill and ephemeral gully erosion. *CATENA* 67, 128–138.
635 <https://doi.org/10.1016/j.catena.2006.03.005>

636 Cerdan, O., Govers, G., Le Bissonnais, Y., Van Oost, K., Poesen, J., Saby, N., Gobin, A., Vacca, A., Quinton,
637 J., Auerswald, K., 2010. Rates and spatial variations of soil erosion in Europe: a study based on
638 erosion plot data. *Geomorphology* 122, 167–177.
639 <https://doi.org/10.1016/j.geomorph.2010.06.011>

640 Cerdan, O., Poesen, J., Govers, G., Saby, N., Le Bissonnais, Y., Gobin, A., Vacca, A., Quinton, J.,
641 Auerswald, K., Klik, A., 2006. Sheet and rill erosion. *Soil erosion in Europe* 501–513.
642 <https://doi.org/10.1002/0470859202.ch38>

643 Chevigny, E., Quiquerez, A., Petit, C., Curmi, P., 2014. Lithology, landscape structure and management
644 practice changes: Key factors patterning vineyard soil erosion at metre-scale spatial resolution.
645 *Catena* 121, 354–364. <https://doi.org/10.1016/j.catena.2014.05.022>

646 De Figueiredo, T., Poesen, J., Ferreira, A.G., 1998. The relative importance of low frequency erosion
647 events: results from erosion plots under vineyards in the Douro region, Northeast-Portugal, in:
648 *Proceedings of the 16th World Congress of Soil Science*. pp. 20–26.

649 Elaoud, A., Chehaibi, S., 2011. Soil Compaction Due to Tractor Traffic. *Journal of Failure Analysis and*
650 *Prevention* 11, 539–545. <https://doi.org/10/bn6cs4>

651 Fressard, M., Cossart, E., 2019. A graph theory tool for assessing structural sediment connectivity:
652 Development and application in the Mercurey vineyards (France). *Science of The Total*
653 *Environment* 651, 2566–2584. <https://doi.org/10.1016/j.scitotenv.2018.10.158>

654 Fressard, M., Cossart, É., Alami, C., Brun, G., Potot, A., Lejot, J., Boulet, R., Christol, A., 2017. Casser la
655 connectivité hydrosédimentaire pour gérer la ressource en sol: cas du vignoble de Mercurey
656 (Bourgogne). *Géomorphologie: relief, processus, environnement*.
657 <https://doi.org/10.4000/geomorphologie.11865>

658 Garcia, J.-P., Labbé, T., Quiquerez, A., 2018. la préservation et la pérennisation des sols viticoles en
659 Bourgogne du Moyen Âge à nos jours, in: J. Pérard & C. Wolikow, dir. (Ed.), *Quelle Durabilité*
660 *En Vignes et En Cave* (J. Pérard & C. Wolikow, Dir.) - *Rencontres Du Clos Vougeot 2017*. Centre
661 *Georges Chevrier et chaire Unesco Culture et traditions du vin*, pp. 51–65.

662 García-Díaz, A., Bienes, R., Sastre, B., Novara, A., Gristina, L., Cerdà, A., 2017. Nitrogen losses in
663 vineyards under different types of soil groundcover. A field runoff simulator approach in
664 central Spain. *Agriculture, Ecosystems & Environment* 236, 256–267.
665 <https://doi.org/10.1016/j.agee.2016.12.013>

666 García-Ruiz, J.M., Beguería, S., Nadal-Romero, E., González Hidalgo, J.C., Lana-Renault, N., Sanjuán, Y.,
667 2015. A meta-analysis of soil erosion rates across the world.
668 <https://doi.org/10.1016/j.geomorph.2015.03.008>

669 Govers, G., Lobb, D.A., Quine, T.A., 1999. Tillage erosion and translocation: emergence of a new
670 paradigm in soil erosion research. *Soil & tillage research*.

671 Greene, R.S.B., Kinnell, P.I.A., Wood, J.T., 1994. Role of plant cover and stock trampling on runoff and
672 soil-erosion from semi-arid wooded rangelands. *Soil Research* 32, 953–973.
673 <https://doi.org/10.1071/SR9940953>

674 Hildebrandt, A., Guillamón, M., Lacorte, S., Tauler, R., Barceló, D., 2008. Impact of pesticides used in
675 agriculture and vineyards to surface and groundwater quality (North Spain). *Water Research*
676 42, 3315–3326. <https://doi.org/10.1016/j.watres.2008.04.009>

677 Kirchhoff, M., Rodrigo-Comino, J., Seeger, M., Ries, J.B., 2017. Soil erosion in sloping vineyards under
678 conventional and organic land use managements (Saar-Mosel Valley, Germany). *Cuadernos de*
679 *Investigación Geográfica* 43, 119–140. <https://doi.org/10.18172/cig.3161>

680 Kosmas, C., Danalatos, N., Cammeraat, L.H., Chabart, M., Diamantopoulos, J., Farand, R., Gutierrez, L.,
681 Jacob, A., Marques, H., Martinez-Fernandez, J., 1997. The effect of land use on runoff and soil
682 erosion rates under Mediterranean conditions. *Catena* 29, 45–59.
683 [https://doi.org/10.1016/S0341-8162\(96\)00062-8](https://doi.org/10.1016/S0341-8162(96)00062-8)

684 Lal, R., 1998. Soil erosion impact on agronomic productivity and environment quality. *Critical reviews*
685 *in plant sciences* 17, 319–464. <https://doi.org/10.1080/07352689891304249>

686 Le Bissonnais, Y., Blavet, D., Noni, G., Laurent, J. -Y, Asseline, J., Chenu, C., 2006. Erodibility of
687 Mediterranean vineyard soils: Relevant aggregate stability methods and significant soil
688 variables. *European Journal of Soil Science* 58, 188–195. [https://doi.org/10.1111/j.1365-](https://doi.org/10.1111/j.1365-2389.2006.00823.x)
689 [2389.2006.00823.x](https://doi.org/10.1111/j.1365-2389.2006.00823.x)

690 Loughran, R.J., Balog, R.M., 2006. Re-sampling for Soil-caesium-137 to Assess Soil Losses after a 19-
691 year Interval in a Hunter Valley Vineyard, New South Wales, Australia. *Geographical Research*
692 44, 77–86. <https://doi.org/10.1111/j.1745-5871.2006.00361.x>

693 Martínez-Casasnovas, J.A., Ramos, M.C., Ribes-Dasi, M., 2005. On-site effects of concentrated flow
694 erosion in vineyard fields: some economic implications. *CATENA* 60, 129–146.
695 <https://doi.org/10.1016/j.catena.2004.11.006>

696 Martínez-Casasnovas, J.A., Ramos, M.C., Ribes-Dasi, M., 2002. Soil erosion caused by extreme rainfall
697 events: mapping and quantification in agricultural plots from very detailed digital elevation
698 models. *Geoderma* 105, 125–140. [https://doi.org/10.1016/S0016-7061\(01\)00096-9](https://doi.org/10.1016/S0016-7061(01)00096-9)

699 Messer, T., 1980. Soil erosion measurements on experimental plots in Alsace vineyards (France). *Soil*
700 *erosion measurements on experimental plots in Alsace vineyards (France)*. 455–462.

701 Morvan, X., Naisse, C., Issa, O.M., Desprats, J.F., Combaud, A., Cerdan, O., 2014. Effect of ground-cover
702 type on surface runoff and subsequent soil erosion in Champagne vineyards in France. *Soil Use*
703 *and Management* 30, 372–381. <https://doi.org/10.1111/sum.12129>

704 Napoli, M., Massetti, L., Orlandini, S., 2017. Hydrological response to land use and climate changes in
705 a rural hilly basin in Italy. *CATENA* 157, 1–11. <https://doi.org/10.1016/j.catena.2017.05.002>

706 Paroissien, J.-B., Lagacherie, P., Le Bissonnais, Y., 2010a. A regional-scale study of multi-decennial
707 erosion of vineyard fields using vine-stock unearthing–burying measurements. *Catena* 82,
708 159–168. <https://doi.org/10.1016/j.catena.2010.06.002>

709 Paroissien, J.-B., Lagacherie, P., Le Bissonnais, Y., 2010b. A regional-scale study of multi-decennial
710 erosion of vineyard fields using vine-stock unearthing–burying measurements. *CATENA* 82,
711 159–168. <https://doi.org/10.1016/j.catena.2010.06.002>

712 Pimentel, D., Harvey, C., Resosudarmo, P., Sinclair, K., Kurz, D., McNair, M., Crist, S., Shpritz, L., Fitton,
713 L., Saffouri, R., 1995. Environmental and economic costs of soil erosion and conservation
714 benefits. *Science-AAAS-Weekly Paper Edition* 267, 1117–1122.

715 Poesen, J., 1993. Gully typology and gully control measures in the European loess belt, in: Wicherek, S.
716 (Ed.), *Farm Land Erosion*. Elsevier, Amsterdam, pp. 221–239. [https://doi.org/10.1016/B978-0-](https://doi.org/10.1016/B978-0-444-81466-1.50024-1)
717 [444-81466-1.50024-1](https://doi.org/10.1016/B978-0-444-81466-1.50024-1)

718 Poesen, J., Ingelmo-Sánchez, F., 1992. Runoff and sediment yield from topsoils with different porosity
719 as affected by rock fragment cover and position. <https://doi.org/10/c4v4x9>

720 Quiquerez, A., Brenot, J., Garcia, J.-P., Petit, C., 2008. Soil degradation caused by a high-intensity
721 rainfall event: implications for medium-term soil sustainability in Burgundian vineyards.
722 *Catena* 73, 89–97. <https://doi.org/10.1016/j.catena.2007.09.007>

723 Quiquerez, A., Chevigny, E., Allemand, P., Curmi, P., Petit, C., Grandjean, P., 2014. Assessing the impact
724 of soil surface characteristics on vineyard erosion from very high spatial resolution aerial
725 images (Côte de Beaune, Burgundy, France). *Catena* 116, 163–172.
726 <https://doi.org/10.1016/j.catena.2013.12.002>

727 Rabiet, M., Margoum, C., Gouy, V., Carluer, N., Coquery, M., 2010. Assessing pesticide concentrations
728 and fluxes in the stream of a small vineyard catchment – Effect of sampling frequency.
729 *Environmental Pollution* 158, 737–748. <https://doi.org/10.1016/j.envpol.2009.10.014>

730 Ramos, M.C., Martínez-Casasnovas, J.A., 2009. Impacts of annual precipitation extremes on soil and
731 nutrient losses in vineyards of NE Spain. *Hydrological Processes* 23, 224–235.
732 <https://doi.org/10.1002/hyp.7130>

733 Remke, A., Rodrigo-Comino, J., Gyasi-Agyei, Y., Cerdà, A., Ries, J., 2018. Combining the stock unearthing
734 method and structure-from-motion photogrammetry for a gapless estimation of soil
735 mobilisation in vineyards. *ISPRS International Journal of Geo-Information* 7, 461.
736 <https://doi.org/10.3390/ijgi7120461>

737 Renard, K.G., Foster, G.R., Weesies, G.A., McCool, D.K., Yoder, D.C., 1997. Predicting soil erosion by
738 water: a guide to conservation planning with the Revised Universal Soil Loss Equation (RUSLE).
739 US Government Printing Office Washington, DC.

740 Reynier, A., 2011. *Manuel de viticulture: guide technique du viticulteur*. Lavoisier.

741 Rodrigo-Comino, J., Brevik, E.C., Cerdà, A., 2018a. The age of vines as a controlling factor of soil erosion
742 processes in Mediterranean vineyards. *Science of the Total Environment* 616, 1163–1173.
743 <https://doi.org/10.1016/j.scitotenv.2017.10.204>

744 Rodrigo-Comino, Jesús, Brings, C., Iserloh, T., Casper, M.C., Seeger, M., Senciales, J.M., Brevik, E.C.,
745 Ruiz-Sinoga, J.D., Ries, J.B., 2017. Temporal changes in soil water erosion on sloping vineyards
746 in the Ruwer-Mosel Valley. The impact of age and plantation works in young and old vines.
747 Journal of Hydrology and Hydromechanics 65, 402–409.

748 Rodrigo-Comino, J., Iserloh, T., Lassu, T., Cerdà, A., Keesstra, S.D., Prosdocimi, M., Brings, C., Marzen,
749 M., Ramos, M.C., Senciales, J.M., Ruiz Sinoga, J.D., Seeger, M., Ries, J.B., 2016a. Quantitative
750 comparison of initial soil erosion processes and runoff generation in Spanish and German
751 vineyards. Science of The Total Environment 565, 1165–1174.
752 <https://doi.org/10.1016/j.scitotenv.2016.05.163>

753 Rodrigo-Comino, J., Quiquerez, A., Follain, S., Raclot, D., Le Bissonnais, Y., Casalí, J., Giménez, R., Cerdà,
754 A., Keesstra, S.D., Brevik, E.C., 2016b. Soil erosion in sloping vineyards assessed by using
755 botanical indicators and sediment collectors in the Ruwer-Mosel valley. Agriculture,
756 Ecosystems & Environment 233, 158–170. <https://doi.org/10.1016/j.agee.2016.09.009>

757 Rodrigo-Comino, J., Senciales, J.M., Ramos, M.C., Martínez-Casasnovas, J.A., Lasanta, T., Brevik, E.C.,
758 Ries, J.B., Ruiz Sinoga, J.D., 2017. Understanding soil erosion processes in Mediterranean
759 sloping vineyards (Montes de Málaga, Spain). Geoderma 296, 47–59.
760 <https://doi.org/10.1016/j.geoderma.2017.02.021>

761 Rodrigo-Comino, J., Cerdà, A., 2018a. Improving stock unearthing method to measure soil erosion rates
762 in vineyards. Ecological indicators 85, 509–517.

763 Rodrigo-Comino, J., Davis, J., Keesstra, S.D., Cerdà, A., 2018b. Updated measurements in vineyards
764 improves accuracy of soil erosion rates. Agronomy Journal 110, 411–417.
765 <https://doi.org/10.2134/agronj2017.07.0414>

766 Rodrigo-Comino, J., Keshavarzi, A., Zeraatpisheh, M., Gyasi-Agyei, Y., Cerdà, A., 2019. Determining the
767 best ISUM (Improved stock unearthing Method) sampling point number to model long-term
768 soil transport and micro-topographical changes in vineyards. Computers and Electronics in
769 Agriculture 159, 147–156. <https://doi.org/10.1016/j.compag.2019.03.007>

770 Salome, C., Coll, P., Lardo, E., Villenave, C., Blanchart, E., Hinsinger, P., Marsden, C., Le Cadre, E., 2014.
771 Relevance of use-invariant soil properties to assess soil quality of vulnerable ecosystems: The
772 case of Mediterranean vineyards. *Ecological Indicators* 43, 83–93.
773 <https://doi.org/10.1016/j.ecolind.2014.02.016>

774 van Dijck, S.J.E., van Asch, Th.W.J., 2002. Compaction of loamy soils due to tractor traffic in vineyards
775 and orchards and its effect on infiltration in southern France. *Soil and Tillage Research* 63, 141–
776 153. <https://doi.org/10/ffbnp4>

777 Verheijen, F.G., Jones, R.J., Rickson, R.J., Smith, C.J., 2009. Tolerable versus actual soil erosion rates in
778 Europe. *Earth-Science Reviews* 94, 23–38. <https://doi.org/10.1016/j.earscirev.2009.02.003>

779 Wischmeier, W.H., Smith, D.D., 1978. Predicting rainfall erosion losses-A guide to conservation
780 planning. *Predicting rainfall erosion losses-A guide to conservation planning*.

781 Zheng, X., Xiong, H., Yue, L., Gong, J., 2016. An improved ANUDEM method combining topographic
782 correction and DEM interpolation. *Geocarto International* 31, 492–505.
783 <https://doi.org/10.1080/10106049.2015.1059899>

784